2008 IEEE Region 10 Colloquium and the Third ICIIS, Kharagpur, INDIA December 8-10, Paper identification number: 641

Impact of Polarization Mode Dispersion and Cross Phase Modulation in a WDM/IM-DD Transmission System

M. S. Islam, *IEEE, Member*
Institute of Information and Communication Technology
Bangladesh University of Engineering and Technology
Dhaka, Bangladesh
E-mail: mdsaifulislam@iict.buet.ac.bd

S. M. Majumder, *IEEE, Member*
Department of Electrical and Electronic Engineering
Bangladesh University of Engineering and Technology
Dhaka, Bangladesh
E-mail: spmajumder@eee.buet.ac.bd

***Abstract*—Cross-phase modulation (XPM) changes the state-of-polarization (SOP) of the channels that leads to amplitude modulation of the propagating waves in a WDM system. Due to the presence of polarization mode dispersion (PMD), the angles between the SOP of the channels change randomly and the modulation amplitude fluctuation in the perturbed channel becomes random. We analytically derive the dynamic equation of the perturbed channel, determine the combined probability density function of the random angle between the SOP of pumps and probe channel and evaluate the impact of PMD on XPM for a 4-channel IM-DD WDM system in terms of BER at bit rate of 10 Gbit/s per channel. We also simulate the interaction PMD and XPM for a 4-chanel WDM system in terms of eye diagram and found that eye opening penalty is 1.85 dB more when the fiber PMD coefficient increases from 0.5 ps/√km to 1.5 ps/ √km.**

Keywords- Cross-phase modulation, Polarization mode dispersion, State-of-polarization, Wavelength division multiplexing, Probability density function.

I. INTRODUCTION

Transmission in optical fiber communication systems is impaired and ultimately limited by the four 'horsemen' of optical fiber communication systems — chromatic dispersion, amplified spontaneous emission noise from amplifier, polarization mode dispersion (PMD) and fiber nonlinearity [1]. Cross-phase modulation (XPM) is a nonlinear phenomenon occurring in optical fibers when two or more optical fields are transmitted through a fiber simultaneously. The nonlinear phase modulation induced through XPM depends on the bit pattern of the inducing channel and is transferred as intensity fluctuation to neighboring channel through group velocity dispersion (GVD) resulting the inter-channel crosstalk. It has an important impact on the performance of high-speed wavelength division multiplexing (WDM) in optical fiber communication systems [2]. In the last few years, many research works have been carried out on the interaction among fiber nonlinearity, polarization variation and PMD [3]-[10]. Physically, PMD has its origin in the birefringence that is present in any optical fiber. Just like signal distortion due to chromatic dispersion and nonlinearity accumulate along the length of the communication link, so does the polarization and PMD. Q. Lin *et al* [5], developed a vector theory of XPM in optical fiber and investigate the effect of PMD on XPM crosstalk in a pump-probe configuration in terms of amplitude of the probe fluctuation induced by a co-propagating pump channel and found that PMD reduces the difference in the average crosstalk level between cases of copolarized and orthogonally polarized channels. G. Zhang *et al* [6], experimentally reported that self phase modulation (SPM) can suppress PMD penalty and XPM-induced polarization scattering in dense WDM transmission systems can also reduce the PMD impairment. R. Khosravani *et al* [7], numerically and experimentally showed that nonlinear polarization rotation can alter the polarization states of the bits that varies from one bit to the next in a way that is difficult to predict and in such cases, conventional PMD compensation becomes impossible. We use Jones-matrix formalism for the electric field evolution and Stokes-vector formalism for SOP of pumps and channel under study on the Poincare sphere.

Due to birefringence in a single mode fiber (SMF), the relative orientation between the pumps and channel under study state-of-polarization (SOP) cause the XPM modulation amplitude to be random. In this paper, first we analytically derive the dynamic equation of the perturbed channel and then determine the probability density function (pdf) of the random combined angle $\theta_j(z)$ between the pumps and channel under study (probe) SOP fluctuation that produce intensity dependent pulse distortion on a propagating signal. Using the pdf we analyzed the impact of PMD on XPM in terms of average bit error rate (BER) for a 4-channel intensity modulation-direct detection (IM-DD) WDM system at a bit rate of 10 Gbit/s per channel. We also simulated the interaction of PMD and XPM for a 4-channel WDM system in terms of eye diagram. To our knowledge the influence of PMD on XPM in terms of BER is yet to be reported in a WDM transmission system.

978-1-4244-2806-9/08/$25.00© 2008 IEEE

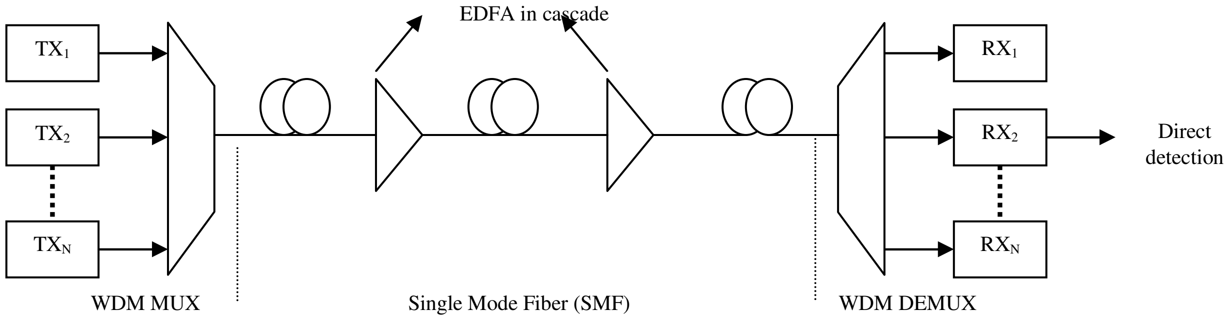

Fig. 1: Block diagram of a WDM system with EDFA in cascade

II. SYSTEM MODEL

The block diagram of a WDM system with EDFA in cascade used for theoretical analysis of PMD and XPM interaction is shown in Fig.1. The different channels are multiplexed by WDM MUX and the composite signal is transmitted through a SMF. To describe the combined effect of PMD on XPM, we assume that except channel 2 all the other channels act as the pump which modulate the transmitted data of channel 2 from the laser diodes at wavelength, λ_j. In this case channel 2 is acts as a probe or channel under study. The in-line EDFA's are used in cascade to compensate the fiber losses. Finally, the composite signal is demultiplexed at WDM DEMUX and from the modulated carrier; wavelength λ_2 original signal (channel 2) is recovered through IM-DD method

III. THEORITICAL ANALYSIS

A. Evolution of Pumps and Probe Field

We assume that the channel under study (channel 2) is weak enough and the SPM, XPM and intrachannel PMD induced by it can be neglected. Although these effects broaden pulse in each channel, they barely affect the interchannel XPM interaction because the channel spacing typically is much larger than channel bandwidth and the evolution of SOP of the channels is mainly governed by the birefringence. The XPM induces a time dependent phase shift as well as nonlinear polarization rotation (NPR) on the probe channel that cause the XPM induced modulation amplitude to be random. To study the temporal modulation of cw channel 2 field as a consequence of all other pump fields, the following equations can be written [5],

$$\frac{\partial|\boldsymbol{A_2}\rangle}{\partial z}=-\beta_{12}\frac{\partial|\boldsymbol{A_2}\rangle}{\partial t}-\frac{i\beta_{22}}{2}\frac{\partial^2|\boldsymbol{A_2}\rangle}{\partial t^2}-\frac{\alpha_2}{2}|\boldsymbol{A_2}\rangle-\frac{i}{2}\boldsymbol{B_2}.\boldsymbol{\sigma}|\boldsymbol{A_2}\rangle + \frac{2i\gamma_2}{3}\sum_j\left[2\langle\boldsymbol{A_j}|\boldsymbol{A_j}\rangle+|\boldsymbol{A_j}\rangle\langle\boldsymbol{A_j}|+|\boldsymbol{A_j^*}\rangle\langle\boldsymbol{A_j^*}|\right]|\boldsymbol{A_2}\rangle \tag{1}$$

$$\frac{\partial|\boldsymbol{A_j}\rangle}{\partial z}=-\beta_{1j}\frac{\partial|\boldsymbol{A_j}\rangle}{\partial t}-\frac{i\beta_{2j}}{2}\frac{\partial^2|\boldsymbol{A_j}\rangle}{\partial t^2}-\frac{\alpha_{j1}}{2}|\boldsymbol{A_j}\rangle -\frac{i}{2}\boldsymbol{B_j}.\boldsymbol{\sigma}|\boldsymbol{A_j}\rangle+\frac{i\gamma_j}{3}\left[2\langle\boldsymbol{A_j}|\boldsymbol{A_j}\rangle+|\boldsymbol{A_j^*}\rangle\langle\boldsymbol{A_j^*}|\right]|\boldsymbol{A_j}\rangle \tag{2}$$

where, we consider the XPM effects on channel 2, while other channels act as the pump ($j \neq 2$). However, both beat length ($L_B \approx 10m$) and correlation length ($L_c \approx 100m$) associated with residual birefringence are much shorter than the nonlinear length ($L_n > 10\,km$, depending on the optical power). As a result, the polarization rotation induced by the residual birefringence is much faster than that induced by NPR. Thus to average over the rapid polarization variation, it is convenient to choose a rotating frame in which the SOP of channel 2 remain frozen. Adopting a rotation frame through a unitary transformation $|\boldsymbol{A_j}\rangle=\vec{\boldsymbol{T}}|\boldsymbol{A_j'}\rangle$, where the Jones matrix $\vec{\boldsymbol{T}}$ satisfies,

$$\frac{d\vec{\boldsymbol{T}}}{\mathrm{dz}}=-\frac{i}{2}\boldsymbol{B_1}.\boldsymbol{\sigma}\vec{\boldsymbol{T}} \tag{3}$$

The unitary matrix $\vec{\boldsymbol{T}}$ in (3) corresponds to random rotations of the Stokes vector on the Poincare sphere that do not change the vector length. After averaging over the rapid variations induced by $\vec{\boldsymbol{T}}$ and using a reduced time variable a $\tau=(t-\beta_{12}z)$, we obtain,

$$\frac{\partial|\boldsymbol{A_2}\rangle}{\partial z}=-\beta_{12}\frac{\partial|\boldsymbol{A_2}\rangle}{\partial\tau}-\frac{i\beta_{22}}{2}\frac{\partial^2|\boldsymbol{A_2}\rangle}{\partial\tau^2}-\frac{\alpha_2}{2}|\boldsymbol{A_2}\rangle -\frac{i}{2}\boldsymbol{B_2}.\boldsymbol{\sigma}|\boldsymbol{A_2}\rangle+\frac{2i\varepsilon_2}{3}\sum_j P_{0j}\left[3+\hat{P}_j.\boldsymbol{\sigma}\right]|A_2\rangle \tag{4}$$

$$\frac{\partial|\boldsymbol{A_j}\rangle}{\partial z}=-\beta_{1j}\frac{\partial|\boldsymbol{A_j}\rangle}{\partial\tau}-\frac{i\beta_{2j}}{2}\frac{\partial^2|\boldsymbol{A_j}\rangle}{\partial\tau^2}-\frac{\alpha_{j1}}{2}|\boldsymbol{A_j}\rangle -\frac{i}{2}\boldsymbol{B_j}.\boldsymbol{\sigma}|\boldsymbol{A_j}\rangle-\frac{i}{2}\Omega_j\boldsymbol{b}.\boldsymbol{\sigma}|\boldsymbol{A_j}\rangle+i\varepsilon_j P_{0j}|A_j\rangle \tag{5}$$

Where, $P_{0j}=\langle\boldsymbol{A_j}|\boldsymbol{A_j}\rangle$ and $\hat{P}_j=\frac{\langle\boldsymbol{A_j}|\boldsymbol{\sigma}|\boldsymbol{A_j}\rangle}{P_{0j}}$ represents the power and the unit Stokes vector of the *j*th channel representing the SOP of the channel on the Poincare sphere. Furthermore, $\Omega_j = (\omega_2 - \omega_j)$ is the channel spacing, $\varepsilon_j = \frac{8}{9}\gamma_j$ and $\varepsilon_2 = \frac{8}{9}\gamma_2$ are effective nonlinear parameters for the jth channel and channel 2 respectively and $\delta\beta_j = (\beta_{1j} - \beta_{12})$ group velocity mismatch between the jth channel and channel 2.

Since, the fiber length (L) is typically much longer than the birefringence correlation length (L_c), we model b_j as a three-dimensional (3-D) stochastic process whose first- and second moments are given by,

$$\langle \boldsymbol{b}_j(z) \rangle = 0\,, \langle \boldsymbol{b}_j(z_1)\boldsymbol{b}_j(z_2) \rangle = \sigma_{\theta j}^2 \delta_j(z_2 - z_1) \qquad (6)$$

Where, $\sigma_{\theta j}^2 = \frac{1}{3} D_p^2 \bar{\boldsymbol{I}}$; $\bar{\boldsymbol{I}}$ is the second-order unit tensor and D_p is the PMD co-efficient of the fiber.

From (4) we see that the pumps (all channels except channel under study) polarization $\hat{P}_j$ remain fixed in the rotating frame. However, PMD changes the relative orientation between the different pumps and channel 2 Stokes vectors at a rate dictated by the magnitude of $\Omega_j \boldsymbol{b}$. The effectiveness of XPM depends not only on the group velocity mismatch $\delta\beta_j$, but also on the relative orientation of all the pumps and channel 2 SOPs.

B. Dynamic Equation of the Perturbed Channel

We shall solve (4) and (5) to study the temporal modulation of channel 2 induced by the combined effect of XPM and PMD of all other channels. Since the modulation amplitude is small in general, we can linearize (4) by assuming that $|\boldsymbol{A_2}\rangle = |\boldsymbol{A_{20}}\rangle + |\boldsymbol{A_{21}}\rangle$, where $|\boldsymbol{A_{20}}\rangle$ and $|\boldsymbol{A_{21}}\rangle$ are unperturbed and perturbed channel 2 fields respectively. Substituting this in (4) we obtain the following two equations governing the evolution of channel 2 field as,

$$\frac{\partial |\boldsymbol{A_{20}}\rangle}{\partial z} = -\frac{\alpha_2}{2}|\boldsymbol{A_{20}}\rangle - \frac{i}{2}\Omega \boldsymbol{b}.\boldsymbol{\sigma}|\boldsymbol{A_{20}}\rangle \qquad (7)$$

$$\begin{aligned}\frac{\partial |\boldsymbol{A_{21}}\rangle}{\partial z} &= -\frac{i\beta_{22}}{2}\frac{\partial^2 |\boldsymbol{A_{21}}\rangle}{\partial \tau^2} - \frac{\alpha_2}{2}|\boldsymbol{A_{21}}\rangle - \\ &\frac{i}{2}\Omega \boldsymbol{b}.\boldsymbol{\sigma}|\boldsymbol{A_{21}}\rangle + \frac{i\varepsilon_2}{2}\sum_j P_{0j}\left[3 + \hat{P}_j.\boldsymbol{\sigma}\right]\boldsymbol{A_{20}}\rangle\end{aligned} \qquad (8)$$

Where the dispersion term for $|\boldsymbol{A_{20}}\rangle$ was set to zero for a cw input of channel 2. The total optical power of the channel 2 field is expressed as,

$$\langle \boldsymbol{A_2} | \boldsymbol{A_2} \rangle \approx \langle \boldsymbol{A_{20}} | \boldsymbol{A_{20}} \rangle + \left[\langle \boldsymbol{A_{20}} | \boldsymbol{A_{21}} \rangle + c.\,c.\right] \equiv \boldsymbol{S_0} + \boldsymbol{\delta S_0} \qquad (9)$$

Here we neglected $\langle \boldsymbol{A_{21}} | \boldsymbol{A_{21}} \rangle$ because of its smallness and introduced the power and SOP of the unperturbed field as,

$$\boldsymbol{S}_0 = \langle \boldsymbol{A_{20}} | \boldsymbol{A_{20}} \rangle \quad \text{and} \quad \hat{\mathrm{S}} = \frac{\langle \boldsymbol{A_{20}} | \boldsymbol{\sigma} | \boldsymbol{A_{20}} \rangle}{\boldsymbol{S}_0} \qquad (10)$$

To find the modulation amplitude $\boldsymbol{\delta S_0}$, which is the measure of the combined PMD and XPM-induced crosstalk, we first find an equation for $\langle \boldsymbol{A_{20}} | \boldsymbol{A_{21}} \rangle$ only. Using (7) and (8), this quantity is found to satisfy the following equation,

$$\begin{aligned}\frac{\partial \langle \boldsymbol{A_{20}} | \boldsymbol{A_{21}} \rangle}{\partial z} &= -\frac{i\beta_{22}}{2}\frac{\partial^2 \langle \boldsymbol{A_{20}} | \boldsymbol{A_{21}} \rangle}{\partial \tau^2} - \alpha_2 \langle \boldsymbol{A_{20}} | \boldsymbol{A_{21}} \rangle \\ &+ \frac{i\varepsilon_2}{2} S_0 \sum_j P_{0j}\left[3 + cos[\theta_j(z)]\right]\end{aligned} \qquad (11)$$

Where, $\theta_j(z) = \hat{P}_j \ \hat{S}(z)$ is the random angle between the different pumps and channel 2 SOPs. Equation (11) can be solved analytically in the frequency domain because of its linear nature. Using $\boldsymbol{\delta S_0} \equiv \langle \boldsymbol{A_{20}} | \boldsymbol{A_{21}} \rangle + \langle \boldsymbol{A_{21}} | \boldsymbol{A_{20}} \rangle$ and introducing the normalized modulation amplitude for the jth channel $\tilde{\delta}_{X_j}(\omega) = \frac{\delta \tilde{S}_0(L, \omega_j)}{S_0(L)}$, where, $\tilde{\delta}_{X_j}(\omega)$ is given by,

$$\tilde{\delta}_{X_j}(\omega) = -\int_0^L \varepsilon_2(z) \tilde{\boldsymbol{P}}_{\boldsymbol{0j}}(z,\omega)\left[3 + cos\theta_j(z)\right] \sin\left[\frac{1}{2}\int_z^L \omega_j{}^2 \beta_{22}(z_1) dz_1\right] dz \qquad (12)$$

Where a tilde denotes the Fourier transform and $\tilde{\boldsymbol{P}}_{\boldsymbol{0j}}(z,\omega)$ is the Fourier spectrum of the different pumps power at a distance z inside the fiber. The effects of PMD enter in this equation through the angle $\theta_j(z)$. More precisely, PMD randomly changes the angle between $\hat{\mathrm{P}}_{\mathrm{j}}$ and $\hat{\mathrm{S}}$ along the fiber and thus makes $\tilde{\delta}_{X_j}(\omega)$ a random quantity. The total modulation amplitude for channel 2 is just the algebraic sum over all pump channels,

$$\tilde{\delta}_X = \sum_j \delta_{X_j}(\omega\ \ ) \qquad (13)$$

To characterize the XPM-induced crosstalk, it is common to introduce the modulation transfer function using the definition,

$$H(L_j, \omega) = \frac{\sum_{j=1}^{L} \langle \tilde{\delta} S_0(L_j, \omega) \rangle}{\tilde{P}(0,\omega)} = \frac{\sum_{j=1}^{L} S_0(L_j)}{\tilde{P}(0,\omega)} \langle \tilde{\delta}_X(\omega) \rangle \qquad (14)$$

C. The Crosstalk Variance, σ_m^2

The total average crosstalk level $\langle \delta_{X_j}(\tau) \rangle_P$ changes with time depending on the bit pattern in the different pump channels. Thus, $\delta_{X_j}(\tau)$ fluctuates with time because of its doubly random nature (*i.e.*, bit pattern and birefringence). In the absence of residual birefringence, randomness comes only from the bit pattern in the pump channels. In this case, it is common to introduce the crosstalk variance, also called PMD and XPM-induced interference, using the following equation,

$$\sigma_j^{\,2} \equiv \frac{1}{T}\int_{-\frac{T}{2}}^{\frac{T}{2}} \left[\delta_{X_j}(\tau)\right]^2 d\tau$$
$$= \frac{1}{4\pi^2}\int_{-\infty}^{\infty} d\omega_j \int_{-\infty}^{\infty} d\omega\; \tilde{\delta}_X(\omega_j)\,\tilde{\delta}_X^{*}(\omega_2)\, sinc\left[\frac{(\omega_j-\omega_2)T}{2}\right] \tag{15}$$

Where, T is the time interval of measurement.

If we assume that bit pattern in different channels are independent of each other, it is easy to show that the variance is also a sum over individual channel such that,

$$\sigma_m^2 = \sum_{j\neq 2}\sigma_j^2 \tag{16}$$

D. Combined PDF and BER Expression

The $\theta_j(z)$ is the sum of all randomly fluctuating angles between the different pumps and the probe channel 2. So, $\theta_j(z)$ can be written as,

$$\theta_j(z) = \theta_1(z) + \theta_2(z) + \theta_3(z) \ldots\ldots\ldots\ldots + \theta_N(z) \tag{17}$$

Since the different pumps polarization $\hat{P}_j$ remain constant and the random variation of $\hat{S}(z)$ (unit vector of the SOP of channel 2) will be responsible for the angle of $\theta_1(z)$.

We have already analytically determined the pdf of $\theta\ (z)$ for a 2 channel (pump-probe configuration), which is given by,

$$p(\theta,z) = \frac{1}{2\pi} + \frac{1}{\pi}\sum_{m=1}^{\infty}\exp(-\frac{1}{2}\eta^2 m^2 z)\cos m(\theta-\theta_0) \tag{18}$$

where, $\theta(z) = .\hat{P}\ \hat{S}(z)$ is the random angle between the pump and probe SOPs and θ_0 is the initial angle.

Now assuming the random variables $\theta_1(z)$, $\theta_2(z)$, $\theta_3(z)$ …. $\theta_N(z)$ are independent and identically-distributed (iid) in nature, then the combined pdf of SOP fluctuation angles for a multi-channel system can be written as the convolution of all the individual random angle that the channel 2 makes with different pumps SOPs (which results (N-2) folds convolution),

$$p_{combined}(\theta,z) = p(\theta_1,z)\otimes p(\theta_2,z)\otimes p(\theta_3,z)\ldots\ldots\ldots p(\theta_N,z) \tag{19}$$

The signal to crosstalk noise ratio (SCNR) can be written as,

$$SCNR = \frac{(R_d S_0)^2}{\sigma_m^2 + \sigma_n^2} \tag{20}$$

where σ_m^2 crosstalk variance due to the combined effect of PMD and XPM of all pump channels, σ_n^2 noise variance, $I_s = R_d S_0$, R_d is the responsivity and S_0 is the affected channel 2 power. Thus,

$$SCNR(for\ angle\quad \theta_0) = \frac{{I_s}^2}{\sigma_m^2(\theta_0) + \sigma_n^2} \tag{21}$$

IV. RESULTS AND DISCUSSION

Following the analytical approach, the performance of a 4-chnnael WDM system is investigated at a bit rate of 10 Gbit/s per channel. Out of 4-channels, we assumed that channel 1, 3 and 4 are pump channel and channel 2 is channel under study, on which we observe the effect of XPM and PMD. The combined pdf, $p_{combined}(\theta,z)$ of the random polarization angle between the pumps and channel 2 is evaluated for various length of the single mode fiber and shown in Fig.2. From the figure, it is noticed that for channel spacing, $\Delta\lambda = 0.8$ nm and at $z = 0$, the pdf results a delta function. The pdf becomes flat (higher variance) as link length increases and the obtained 4-channel random angle pdf is more close to the normal distribution.

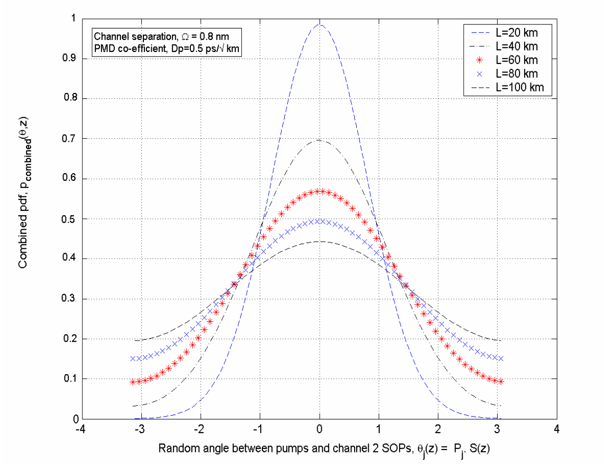

Fig. 2: Plots of pdf of $\theta_j(z) = \hat{P}_j\,.\hat{S}(z)$ at different length of fiber link

The average BER vs pump power is plotted in Fig.3 for different channel spacing. We use the wavelengths from 1549.4 nm to 1552.8 nm to accommodate the 4-cahnnels. It is observed that the impact of PMD and XPM increases as the channel spacing decreases for specific pump power. For example, when the total pump power is 0 dBm, channel 2 BER is about 10^{-6} and 10^{-10} at channel spacing of 2 nm and 3 nm respectively. However, at increased pump power the BER increases and when pump power is about 18 dBm the BER curves makes a floor at 10^{-1} irrespective of channel spacing.

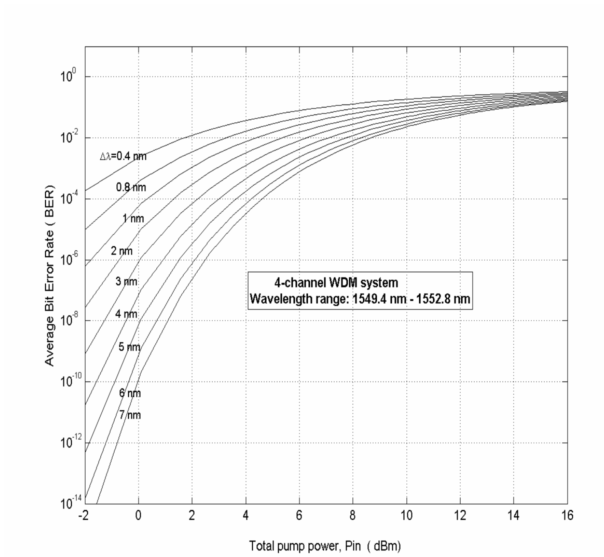

Fig.3: Plots of average BER vs pump power for different channel spacing

To evaluate the effect XPM and PMD on channel under study, we vary the channel 2 power from -2 dBm to 16 dBm and the results of this evaluation is shown Fig. 4. It is found that at relatively high pump and for channel 2 fixed input power, the BER performance deteriorates sharply. It happens due to the strong interaction of PMD and XPM. For example, when the pump power (each channel) is -15dBm, we can achieve of BER 10^{-10} for a power of 8 dBm of channel 2. Keeping the channel 2 power constant, it is observed that at 20 dBm pumps power the BER drops to 10^{-1} only. This deterioration happens due to the higher modulation amplitude fluctuation as a result of high pump power.

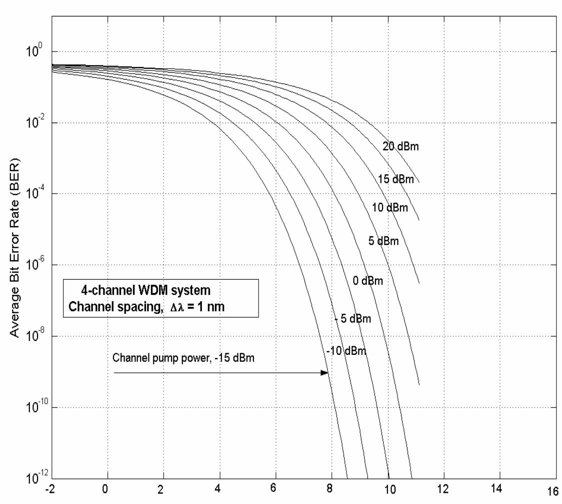

Fig. 4: Plots of average BER vs channel 2 power for different pumps power

The transfer function for amplitude fluctuation of channel 2 is derived in (14). We evaluate the average amplitude fluctuations for 3-different channel spacing (in wavelength) as a function of fiber link length and shown in Fig.5. It is seen from the figure that for higher channel spacing the crosstalk is less or minimum. For example, at 100 km the amount of average amplitude fluctuation or crosstalk is -33 dB, -27 dB and -23 dB for channel spacing of 4 nm, 1 nm and 4 nm respectively.

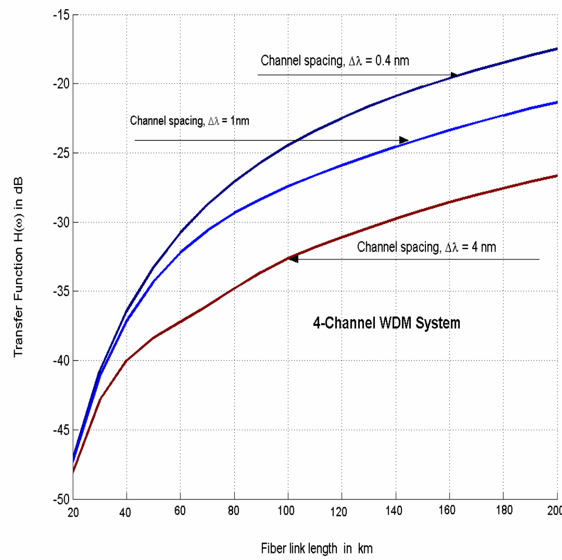

Fig. 5: Average amplitude transfer function vs fiber link length

We carried out simulation of the interaction between PMD and XPM for a 4-channel WDM system in presence of chromatic dispersion. The channels are modulated at 10 Gbit/s data rate using NRZ format and separated by 1 nm and the distance between the inline optical EDFA fiber amplifiers is 100 km (span length). To assess the impact of XPM and PMD on channel in electrical domain we monitor the eye diagram of the channels at the input (back-to-back) as well as at the output for a receiver sensitivity of -24 dBm (at a BER of 10^{-9}). Fig.6 shows the eye diagrams at the input and output of the fiber link of different channels for PMD coefficients of 0.5 ps/√km and 1.5 ps/√km.

It is observed that for a fixed channel space (1nm in this case) the channel 2 eye diagram deteriorates more at 1.5 ps/√km than that of 0.50 ps/√km and other channels are also affected due the high value of PMD coefficient. We may calculate the average eye opening penalty (EOP) due to PMD and XPM in channel 2. Here, we define the parameter of the eye-opening penalty (EOP) as

$$EOP = -20\log\left(\frac{B}{B_0}\right) \tag{22}$$

where, B is the eye opening without PMD effect and B_0 is the eye-opening with PMD and XPM in channel 2. In this case, it is found that the EOP (at a probability of 10^{-3}) at PMD coefficient 1.5 ps/√km is about 1.85 dB more than that of 0.5 ps/√km.

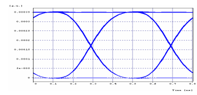

(a)

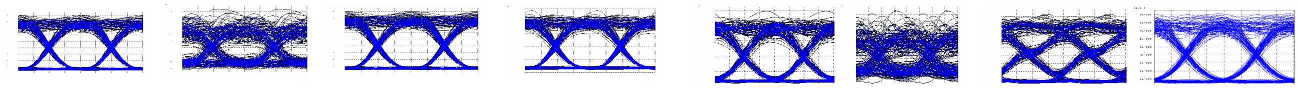

Ch 1 Ch 2 Ch 3 Ch 4 Ch 1 Ch 2 Ch 3 Ch 4

(b) **(c)**

Fig. 6: (a) Base line eye diagram (back-to-back), (b) Channel 1- 4 at the output for a PMD coefficient of 0.5 ps/√km; (c) Channel 1- 4 at the output for a PMD coefficient of 1.5 ps/√km

.

The Plots of bit error rate (BER) vs input pump power is shown in Fig.7. It is observed that the maximum interaction occurs between XPM and PMD at zero dispersion co-efficient (*i.e.*, the BER is significantly higher) and as the dispersion coefficient increases the effect is less due to the walk-off phenomenon. On the other hand, as pump power increases the BER decreases due to the larger effect of PMD and XPM

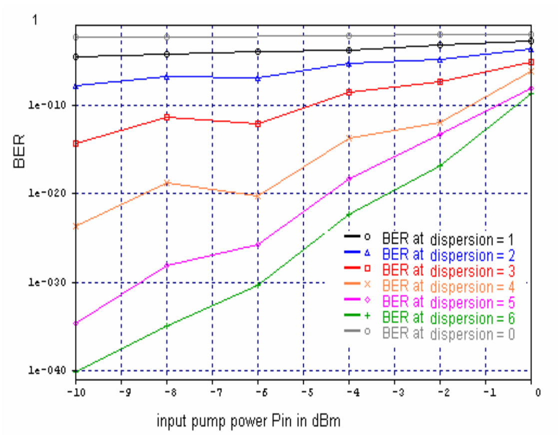

Fig. 7: BER vs input pump power for chromatic dispersion coefficient (dispersion) , $D_c = 0$ ps/nm-km - 6 ps/nm-km

V. Conclusion

In this research work, we have developed a vector theory of XPM and PMD interaction phenomenon that occurs inside optical fibers using the Jones-matrix formalism for a WDM transmission system. We applied the theory for a 4-channel WDM system in which channel 2 in which the week cw signal is perturbed by other 3 co-propagating channels. The birefringence fluctuations responsible for PMD change the relative orientation $\theta_j(z)$ between the pumps and channel 2 Stokes vectors. It is shown that changes in $\theta_j(z)$ affect the XPM interaction among the various channels and PMD induced XPM crosstalk becomes polarization independent when channel spacing is large (*i.e.*, > 4 nm).

We have also demonstrated the interaction of PMD and nonlinear SMF effect XPM by Rsoft OptSim simulation software in a 4-channel WDM system in terms of eye diagram and BER. We show that PMD changes the XPM efficiency and affects the interference condition among the XPM-induced nonlinear phase shifts in different sections of the fiber link.

References

[1] G. P. Agrawal, Nonlinear Fiber Optics, San Diego, CA, Academic Press, 2001.

[2] P. I. Killey, H. J. Thiele, V. Mikhailove and P. Bayvel, "Prediction of transmission penalties due to cross-phase modulation in WDM systems using simplified Technique', *IEEE Photon. Technol. Lett.*, vol.12, no. 7, pp. 804-806, 2007.

[3] N. Hanik "Influence of polarization mode dispersion on the effect of cross-talk modulation in optical WDM transmission", *Proc. of the 6th International Conference on Transparent Optical Networks,* vol.1, pp. 90-194, 2004.

[4] A. Bononi, A. Vanocci, A. Orlandini, E. Corbel, S. Lanne and S. Bigo, "Degree of polarization degradation due to cross-phase modulation and its impact on polarization mode dispersion", *J. Lightwave Technol.*, vol. 21, no. 19, pp.1903-1913, 2003.

[5] Q. Lin and G. P. Agrawal, "Effects of polarization mode dispersion on cross-phase modulation in dispersion managed wavelength-division-multiplexed systems", *J. Lightwave Technol.*, vol.22, no. 4, pp. 977-987, 2004.

[6] G. Zhang, J. T. Stango, X. Zhang and C. Xie, "Impact of fiber nonlinearity on PMD penalty in DWDM transmission systems," *IEEE Photon. Technol. Lett.*, vol. 17, no. 2, pp. 501-503, 2005.

[7] C. R. Menyuk and B. S. Mark, "Interaction of polarization mode dispersion and nonlinearity in optical fiber transmission systems", *J. Lightwave Technol.*, vol.24, no.7, pp. 2806-2826 , 2006.

[8] R. Khosravani, Y. Xie, L. -S. Yan, A. E. Willner and C. R. Menyuk, "Bit pattern dependent polarization rotation in the first-order PMD-compensated WDM systems", *Optics Communications*, pp. 191-196, 2005.

[9] L. Moller, Y. Su, G. Raybon, S. Chandrasekar and L. L. Buhl, "Penalty interference of nonlinear intra-channel effect and PMD in ultra-high speed TDM systems", *Electron Lett.*, vol. 38, no. 6, pp. 281-283, 2002.

[10] P. K. A Wai and C. R. Menyuk, "Polarization mode dispersion, decorrelation and diffusion in optical fibers with randomly varying birefringence," *J. Lightwave Technol.*, vol. 14, no.2, pp.148-157, 1996